# Accepted Manuscript

# Poly(ionic liquid) thermo-responsive hydrogel microfluidic actuators

By *Alexandru Tudor[†a], Janire Saez[†b], Larisa Florea[a*], Fernando Benito-Lopez[b*] and Dermot Diamond[a]*

[a]Insight Centre for Data Analytics, National Centre for Sensor Research, Dublin City University, Dublin 9, Ireland.

[b]Analytical Microsystems & Materials for Lab-on-a-Chip (AMMa-LOAC) Group, Microfluidics UPV/EHU Cluster, Analytical Chemistry Department, University of the Basque Country UPV/EHU, Vitoria-Gasteiz, Spain.

†Authors contributed equally to this work

*Corresponding author E-mail: larisa.florea@dcu.ie, fernando.benito@ehu.eus

**Highlights**
- Poly(ionic liquid) microfluidic-integrated actuators are reported for the first time.
- PIL hydrogels are based on tributylhexyl phosphonium sulfopropylacrylate.
- PIL hydrogel size is modulated by localised changes in temperature.
- PIL hydrogels show repeatable performance as thermo-actuated flow controllers.
- Hydrogel shrinks by ~56 % in area when the temperature is raised from 20 to 70 °C.

**Abstract**

In this study we report the synthesis, characterisation and performance of thermo-responsive crosslinked tributylhexyl phosphonium sulfopropylacrylate (PSPA) poly(ionic liquid) (PILc) hydrogels as temperature controlled actuators in microfluidic devices. The hydrogel size is modulated by localised changes in its temperature due to the lower critical solution temperature (LCST) behaviour exhibited by PSPA.

Keywords: (Microfluidics, Actuators, Smart Materials, Temperature Responsive Materials, Ionic Liquids, Poly(ionic liquid)s)

## 1. Introduction

Microfluidics is an interdisciplinary science that focuses on producing devices capable of manipulating small volumes of fluids, ranging from picoliters to microliters [1, 2]. The advantages of microfluidics come either directly from the reduction in size compared to conventional laboratory fluidics or as a result of the ability to integrate sequential processes at the micro-scale. The former results in reduced reagent consumption, low waste production, reduced measurement times and improved sensitivity, while the latter offers the benefits of sampling, pre-processing and sample analysis "on-chip", thereby reducing process time, risk of contamination, and human error[1-10]. Despite many years of research, functioning devices incorporating microfluidics still typically require highly specialised and bulky macroscopic equipment such as pumps, valves and detectors to be located off-chip. Therefore, one of the main challenges in microfluidics is downscaling conventional pumps and valves so they can be fully integrated within the microfluidic device. In this context, one of the approaches that are being explored is the use of soft materials for flow control[11-17]. In recent years, effective fluidic control systems based on soft, polymer gel-type materials fully integrated within the microfluidic device have been demonstrated by several groups. These novel devices are now becoming more reminiscent of biological units than conventional silicon micromachined components. Examples include the microfluidic integration of a variety of stimuli-responsive materials that respond to changes in their external environment, such as temperature, light, pH, or variations in electrical potential and pressure[18-32]. Among them, one of the most studied stimuli-responsive hydrogels is poly(N-isopropyl acrylamide) (pNiPAAm), due to its lower critical solution temperature (LCST) behaviour in the presence of an aqueous medium[20, 33-35]. LCST behaviour arises from changes in the hydration forces between the polymer chains and the aqueous medium, and the attractive forces between the polymer chains themselves. If the temperature of the hydration medium is below the LCST, then the

polymer chains are hydrated and swollen by the aqueous medium. When the temperature rises above the LCST, the polymer chains expel the water molecules and attract each other, which leads to the polymer collapsing from solution and contraction of the polymer[20, 33-35]. In the case of a linear polymer, the presence of a LCST leads to the appearance of a polymer precipitate, while in the case of a crosslinked polymeric hydrogel, it causes volume contraction[31, 34]. This property has made pNiPAAm hydrogels interesting candidates for the realisation of thermo-responsive microfluidic valves and for thermo-, photo-[36], magneto-responsive valving units when ionic liquids[37], photochromic molecules[14, 38], or magnetic nanoparticles[39, 40], respectively, are included in the polymer matrix.

Similar LCST behaviour has been reported recently in a relatively new class of materials, namely poly(ionic liquid)s (PILs)[22, 29-31, 41-43]. These materials are polymers formed through the polymerisation of ionic liquid (IL) monomers which feature a polymerisable group in the anion, the cation or both. Although generally the focus remains on linear PILs, there are several reports dealing with crosslinked PIL networks, that are explored either as ion conductors[44, 45], templates for multilamellar structured nanoparticles[46] or as actuators[31, 47].

The aim of this paper is the integration, for the first time, of the phosphonium-based crosslinked PIL tributylhexylphosphonium sulfopropylacrylate (PSPA), in a microfluidic structure, to provide thermo-actuated flow control functionality.

## 2. Materials and Methods

### 2.1 Materials and reagents

Potassium 3-sulfopropyl acrylate (KSPA),  2-hydroxy-2-methylpropiophenone 97% (HMPP), phenyl-bis(2,4,6-trimethylbenzoyl) phosphine oxide 97% (PBPO), polypropylene glycol diacrylate ($M_w$ ~800, 100 ppm MEHQ and 100 ppm BHT as inhibitors) (PPG800) and HPLC grade acetonitrile (ACN) were bought from Sigma Aldrich® (Arklow, Ireland) and

used as received. Tributylhexyl phosphonium chloride was kindly donated by Cytec®

Industries (Niagara Falls, Canada). Deionized water (DI water), with a resistivity of 18.2

MΩ·cm⁻¹, was made using a Milli-Q Water Purification System (Merck Millipore,

Darmstadt, Germany).

**2.2 Synthesis of the tributylhexyl sulfopropyl acrylate (PSPA) ionic liquid monomer**

For PSPA synthesis, 15g of tributylhexyl chloride (PCl) and 16.02g of KSPA were

dissolved in 25 mL DI water. The amount of KSPA used represents a 50% molar excess

compared to the stoichiometric value needed for this reaction. This was done to ensure that

the reaction equilibrium is shifted towards the formation of PSPA. The reaction was

maintained at room temperature and atmospheric pressure overnight (Scheme 1). Purification

was done by extracting the PSPA from the aqueous solution with dichloromethane. This

process was repeated three times. The resulting mixture was dried over anhydrous

magnesium sulphate and gravity filtered. Following this, the extraction solvent was removed

by rotary evaporation and the resulting viscous mixture was dried overnight using a high

vacuum pump. The obtained product was a clear, colourless viscous liquid. The yield of the

synthesis was 85%. The purity of the product was analysed using ¹H-NMR, δH (Bruker

Advance Ultrashield, 400MHz, deuterated chloroform): 0.86–1 (m, 12H, $CH_3$), 1.28–1.33 (m,

4H, $CH_2$), 1.51–1.53 (m, 16H, $CH_2$), 2.18–2.37 (m, 10H, $CH_2$), 2.88–2.92 (m, 2H, $CH_2$),

4.25–4.29 (t, J=6.46 Hz, 2H, $CH_2$), 5.77–5.80 (dd, 1H, J=1.51, 10.42 Hz, CH), 6.04–6.11 (m,

1H, J=10.44, 17.33 Hz, CH), 6.34–6.39 (dd, 1H, J= 1.51, 17.38 Hz, CH) ppm.

**2.3 Crosslinked PSPA hydrogel disk polymerization**

The crosslinked PILc hydrogel was synthesized by dissolving 0.1935 g (400 μmols)

of PSPA in 0.1935 g 1:1 w/w mixture of ACN and DI water together with 0.0160 g (20

μmols) of PPG800 as the crosslinker and 0.0034 g (8 μmols) of PBPO as the photo-

polymerization initiator. The resulting mixture was mechanically stirred until all the components were completely dissolved. Following this, the monomer solution was pipetted in poly(dimethyl siloxane) moulds 3mm wide and 1mm deep (Fig. 1). To polymerize the monomer mixture, a Dolan-Jenner LMI-6000 Fiber-Lite (Boxborough, MA, USA) white-light was used at an illumination level of ~200 kLux for 30 minutes. The resulting PILc disks were swollen in DI water overnight (Fig. 1). Based on previously done studies [48], a polymerisation time of 30 minutes ensures that the monomer mixture is fully polymerised.

**2.4 Characterization of the temperature-induced shrinking/reswelling of the hydrogel disks**

The resulting hydrogel disks, as seen in Fig. 1, were transferred to an Anton Paar MCR301 rheometer fitted with a Peltier temperature control holder with an aluminium plate. The hydrogel disks were covered with DI water and the holder was covered with a 5mm glass plate, to ensure that the water will not evaporate when the temperature was raised. Two different experiments were performed: the first experiment focused on the study of the shrinking and swelling kinetics of the hydrogel disks, while the second experiment focused on the repeatability and the reproducibility of the shrinking and reswelling effect. The first experiment was carried out by heating the hydrogels from 20 °C to 70 °C in 5 °C steps to analyze the shrinking effect, followed by cooling the gels at the same rate back to 20 °C to analyze the reswelling effect. The hydrogel disks were kept for 8 minutes at each step to ensure that the area of the hydrogel has reached a steady state. At each step an image was taken using an Aigo GE-5 digital microscope having a 60x magnification objective. The hydrogels' %shrinking in area was studied using the ImageJ software. Each image was analyzed using the following formula:

$$\%\text{shrinking} = 100 - (A_f/A_i \cdot 100) \qquad\qquad \text{(Eq. 1)}$$

Where $A_f$ is the size of the shrunken hydrogel disk at a set temperature and $A_i$ is the initial size of the swollen hydrogel disk.

To further illustrate this behaviour, a time-lapse video of the gel shrinking and reswelling was made by using images taken every 20 seconds for a total of 60 minutes for each shrinking and reswelling cycle (Video : Temperature-induced shrinking and reswelling of PILc hydrogels). The second experiment was done by alternatively shrinking the hydrogel disks by applying a temperature of 50 °C and reswelling them by applying a temperature of 20 °C. This alternation was repeated six times to ensure that the temperature-induced shrinking behaviour is repeatable. The same formula (Eq. 1) was used in this case to calculate %shrinking in area when the hydrogels were heated to 50 °C.

### 2.5 Microfluidic chip fabrication

The microfluidic chip was fabricated from poly(methyl methacrylate) (PMMA) sheets with a height of 250 μm and pressure sensitive adhesive (PSA) sheets with a thickness of 60 μm. The bottom parts of the chip, the well layer in which the hydrogel was polymerized and the top part of the chip were cut using an Epilog Zing 16 30W $CO_2$ laser. These three PMMA layers were bound using two PSA layers, the first of which was used to connect the bottom part of the chip to the polymer well layer of the chip, while the second PSA layer had the microfluidic channel cut into it and was used to connect the top part of the chip to the polymer well layer of the chip (Fig. 2). The PSA layers were cut using a Graphtec Craft Robo-Pro cutting plotter. The total thickness of the chip upon assembly (Fig. 3) was 1 mm. This dimension was used to ensure the chip will fit in the microfluidic chip holder which will be used to actuate the thermo-responsive hydrogel actuator.

## 2.6 Thermo-responsive hydrogel actuator characterization

The hydrogel actuators were fabricated by photo-polymerising 3 µL of monomer mixture for 20 min using a 365nm UV lamp. In this case, the PBPO initiator was substituted, while respecting the same mol ratio, with HMPP to allow UV photopolymerisation. Based on a previously published study[49], the polymerisation time used ensures the full monomer conversion. The characterization of the hydrogel actuator's thermo-response was done by inserting the microfluidic chip into a microfluidic holder fitted with a heating element. This heating element sits at the bottom of the microfluidic chip and is capable of homogenously increasing the temperature at a rate of 7.4 $°C·s^{-1}$ and decreasing the temperature at a rate of 2.4 $°C·s^{-1}$. To induce shrinking in the thermo-responsive PILc hydrogel, a temperature of 50 °C was chosen, while to reswell the hydrogel a temperature of 20 °C was chosen.  The microfluidic holder also contains the inlet and outlet connections at its sides. After the microfluidic chip was placed in the holder, its inlet was connected to a WPI-Europe SP101IZ syringe pump, while its outlet was connected to a Sensirion CMOSens flow microsensor. The flow rate was set at 500 $nL·min^{-1}$. The schematic of the setup can be seen in Scheme 2.

DI water was chosen as the flow medium to ensure that there are no other effects inhibiting the shrinking behaviour of the PIL hydrogels. The effect of foreign salts dissolved in the hydration medium on the temperature-induced shrinking of both linear and crosslinked PILs were investigated in several other studies[18, 28, 29, 48, 50]. For future applications envisioned to work with different kinds of solutions as flow mediums, a configuration in which the hydrogel flow control actuator is separated from the flow medium by a flexible membrane can be used, as demonstrated by Tanaka *et. al*[51] and Beebe *et. al*[11] . In both cases they used a flexible membrane to separate an electroactive polymer, and a pH-responsive hydrogel, respectively, from the analyte flow, which ensured that they operated in optimal conditions.

The results exhibited by the ionic liquid polymer flow control actuator followed a sigmoidal fit (Flow rate, $Q$, *versus* time, $t$) (Eq.2). This type of fit is commonly used in chemistry to obtain constant values such as $pK_a$ (acid dissociation constant) and can be used to determine the rate constant of the ionic liquid polymer hydrogel actuator in this case.

$$Q = \frac{a}{1 + e^{kx+b}} + d \qquad\qquad \text{(Eq. 2)}$$

Where "$a$" is the maximum $Q$ value obtained when hydrogel is fully open, "$b$" correspond to the interception point value, $k$ give us the value of the rate constant, and "$d$" accounts for a baseline offset, minimum $Q$.

Using the setup from Scheme 2 the flow rates through the chip were analysed. Based on these results, further investigations were made to determine the shrinking and swelling kinetics by using the logistic curve equation and the Solver plug-in for Microsoft Excel (Eq. 2). In Fig. S1 and S2 (ESI) detailed views of the flow rate and the modelled flow rate can be seen.

## 3. Results and Discussion

### 3.1 Temperature response of the hydrogel disks

In the case of conventional temperature-responsive linear polymers, such as poly(N-isopropylacrylamide), the LCST appears as a sharp transition at a specific temperature value (~ 32 °C for pNiPAAm)[34]. This remains valid also for linear PILs. In contrast, with crosslinked PILs the polymeric volume changes occur over a temperature interval, rather than at a sharp value, suggesting that more gradual changes are occurring in the polymer chains[31]. This phenomenon has been assigned to the decreased level of freedom of the bulky IL in the polymer network and manifests itself in an incremental decrease in size of the PIL hydrogels

with increase in temperature (and vice versa). This behaviour also appears to occur in the PSPA hydrogels presented in this study.

Figure 4 shows that when the temperature is increased from 20 °C to 70 °C the hydrogels shrink by ~ 39 % at 50 °C and ~56 % at 70 °C (Video S1). When the temperature is lowered back from 70 °C to 20 °C, the hydrogels start absorbing water until they return to their original size. The slight difference in area between the heating and the cooling cycle arose from the fact that the heating rate is ~ 10 °C·min$^{-1}$, while the cooling rate is ~ 13 °C·min$^{-1}$.

Figure 5 presents results of reproducibility and repeatability of this behaviour. In these experiments, a set of three gels were analysed by heating their hydration medium to a temperature of 50 °C to make the hydrogels shrink, followed by cooling them to 20 °C to allow for reswelling to their original size. As in the previous test, the hydrogels were kept for 8 min at each temperature, to ensure a steady-state volume was reached. The heating and cooling cycle was repeated six times. In all cases the hydrogels shrank by ~ 44 % (± 3 %, n = 6) at 50 °C and reverted back to ~ 97 % (± 2 %, n = 6) of their original size when the temperature was lowered to 20 °C.

**3.2 Flow characterization study**

Following this, microfluidic devices were fabricated as described in the experimental section with the necessary configuration for a hydrogel to be photopolymerised and used as a temperature-controlled actuator. The hydrogel actuator was opened and closed six times (Fig. 6), thus confirming the reproducibility and repeatability of the PIL hydrogel thermo-actuation.

In the 'open' form, when the actuator is fully contracted, a flow of ~120 nL min$^{-1}$ occurs rather than the 500 nL min$^{-1}$ flow rate obtained with a fully open channel. This means that the PIL actuator is partially occluding the microchannel, impeding the normal flow through the microchannel. In the actuator's "closed" form, the flow sensor still detects a residual flow of 20 nL min$^{-1}$ rather than 0. The reason why the flow signal does not reach 0 nL min$^{-1}$ can be attributed to small residual pathways through which the fluid still can pass:

(1) either bypassing the swollen gel (*e.g.* where the gel meets the channel top surface); or

(2) through the valve structure (due to pores or inherent liquid transport arising from the open polymeric structure of the hydrated gel).

Both of these effects can be corrected by changing the geometry of the hydrogel actuator, together with design optimizations of the microfluidic device. Moreover, the PIL hydrogel can be placed behind a thin elastic membrane, to ensure that the hydrogel does not come into contact with the liquid flowing through the microfluidic device if the application deems it necessary. Furthermore, with additional optimization, the PIL materials could be used either as valves in simple, low-cost, microfluidic platforms, or as temperature-modulated flow regulators, due to their wide LCST interval. This property can be used to affect the measured flow through a microfluidic device in a repeatable and reproducible way, thus providing enough information for a pulse width modulation feedback loop platform to control the flow through a microfluidic device automatically. In addition, to better understand the ability of this hydrogel actuator to be used in a microfluidic device, its burst pressure was determined. This was done by applying incremental increases in pressure to the hydrogel actuator starting with 5 mbar up to 400 mbar (Fig. S3). When the pressure reached the value of 250 mbar, the hydrogel actuator started degrading, which resulted in an increase in flow rate (time: 1860s). At 400 mbar, complete failure of the hydrogel actuator was observed. Consequently, based on

the results obtained for this particular microchip configuration, the burst pressure was acknowledged to be 250 mbar, while the complete failure pressure was found to be 400 mbar. The shrinking and swelling rate constants of the hydrogel actuator (Table 1) were calculated using the logistic curve equation (Eq. 2) based on the flow rate measurements (Fig. 6).

The rate constants were found to be $(1.1 \pm 0.3) \cdot 10^{-2}$ s$^{-1}$ (n = 6) for the shrinking of the hydrogel and $(1.1 \pm 0.5) \cdot 10^{-2}$ s$^{-1}$ (n = 5) for the swelling of the hydrogel. The close values of the rate constants convey the fact that both effects take place with approximately the same speed, which indicates no perceptible hysteresis between the opening and the closing of the PILc hydrogel flow regulator when the temperature was cycled between 50 °C and 20 °C (SI, Fig. S1 and Fig. S2). This effect is confirmed by the fact that the closing and opening time of the hydrogel actuator vary between 5 to 8 s. The actuation time values compare favourably with actuation times given for other stimuli-responsive hydrogels actuators based on conventional thermo-responsive polymers[52], or several phase-change mechanical actuators based on paraffin wax[6], while being similar with state of the art in hydrogel valves[37, 53]. Compared to other type of actuators, especially vacuum operated or electrically operated hard valves, the response times are slower. Regardless of this, there are several ways in which their response times could be improved, including: fitting a heating element capable of much faster heating and cooling rates, changing the geometry of the hydrogel and the hydrogel positioning to ensure that there is a need for less hydrogel to open and close the microchannel, and the addition of a pore forming agent to the monomer mixture, such as high molecular weight poly(ethylene glycol), which would help the hydrogel absorb and expel its hydration medium faster[54].

**4. Conclusion**

In conclusion, a tributylhexyl phosphonium sulfopropyl acrylate ionic liquid monomer was synthesised and photopolymerised to produce a poly(ionic liquid) hydrogel that features a lower critical solution temperature. Due of this, the hydrogel is able to shrink by increasing the temperature of its surrounding hydration medium. Based on this thermo-responsive behaviour, the hydrogel actuation behaviour was fully characterised and the hydrogel was incorporated into a microfluidic device with the purpose of being used as temperature-controlled actuator. The characterisation of the hydrogel indicates that the hydrogel shrinks by ~ 58 % of its swollen area when the temperature is raised from 20 to 70 °C and ~ 39 % when the temperature is raised from 20 to 50 °C. Furthermore, the hydrogel is able to shrink and reswell repeatedly when subjected to temperature cycles between 20 °C and 50 °C. Moreover, by including the hydrogel in a microfluidic device as a temperature-controlled actuator, the microfluidic channel was modulated between ~ 110 $nL \cdot min^{-1}$ ($\pm$ 15 $nL \cdot min^{-1}$, n = 6) and ~ 27 $nL \cdot min^{-1}$ ($\pm$ 5 $nL \cdot min^{-1}$, n = 6) by varying the temperature between 50 °C and 20 °C. This process was repeated six times with no performance loss, thus suggesting the possibility of repeatable use for more than six times. Based on these results and taking into account the vast collection of ionic liquids available and their synthetic versatility, thermo-responsive poly(ionic liquid)s could constitute a new tool box for the generation of simple and low-cost temperature responsive microfluidic actuators.

## References

1.  P. N. Nge, C. I. Rogers and A. T. Woolley, *Chemical Reviews*, 2013, **113**, 2550-2583.
2.  G. M. Whitesides, *Nature*, 2006, **442**, 368-373.
3.  L. Dong and H. Jiang, *Soft Matter*, 2007, **3**, 1223.
4.  I. Araci and P. Brisk, *Current Opinion in Biotechnology*, 2014, **25**, 60-68.
5.  M. I. Mohammed, E. Abraham and M. P. Y. Desmulliez, *Journal of Micromechanics and Microengineering*, 2013, **23**, 35034.
6.  S. Ogden, L. Klintberg, G. Thornell, K. Hjort and R. Bodén, *Microfluidics and Nanofluidics*, 2014, **17**, 53-71.
7.  K. W. Oh and C. H. Ahn, *Journal of Micromechanics and Microengineering*, 2006, **16**.
8.  P. Selvaganapathy, E. T. Carlen and C. H. Mastrangelo, *Sensors and Actuators A: Physical*, 2003, **104**, 275-282.
9.  B. Yang and Q. Lin, *Sensors and Actuators A: Physical*, 2007, **134**, 194-200.
10. C. Zhang, D. Xing and Y. Li, *Biotechnology Advances*, 2007, **25**, 483-514.
11. D. J. Beebe, J. S. Moore, J. M. Bauer, Q. Yu, R. H. Liu, C. Devadoss and B.-H. Jo, *Nature*, 2000, **404**, 588-590.
12. A. K. Agarwal, L. Dong, D. J. Beebe and H. Jiang, *Lab on a Chip*, 2007, **7**, 310-315.
13. L. Florea, D. Diamond and F. Benito-Lopez, *Research Perspectives on Functional Micro-and Nanoscale Coatings*, 2016, 265.
14. J. ter Schiphorst, S. Coleman, J. E. Stumpel, A. Ben Azouz, D. Diamond and A. P. Schenning, *Chemistry of Materials*, 2015, **27**, 5925-5931.
15. B. Ziółkowski, M. Czugala and D. Diamond, *Journal of Intelligent Material Systems and Structures*, 2012, 1045389-12459591.
16. M. Czugala, C. O'Connell, C. Blin, P. Fischer, K. J. Fraser, F. Benito-Lopez and D. Diamond, *Sensors and Actuators B: Chemical*, 2014, **194**, 105-113.
17. J. Saez, J. Etxebarria, M. Antoñana-Diez and F. Benito-Lopez, *Sensors and Actuators B: Chemical*, 2016, **234**, 1-7.
18. Y. Men, X.-H. Li, M. Antonietti and J. Yuan, *Polymer Chemistry*, 2012, **3**, 871.
19. R. Bogue, *Assembly Automation*, 2012, **32**, 37.
20. C. Boutris, E. G. Chatzi and C. Kiparissides, *Polymer*, 1997, **38**, 2567-2570.
21. L. Florea, D. Diamond and F. Benito‐Lopez, *Macromolecular Materials and Engineering*, 2012, **297**, 11481159.

22. S. Gallagher, L. Florea, K. J. Fraser and D. Diamond, *International Journal of Molecular Sciences*, 2014, **15**, 5337-5349.

23. S. Gallagher, A. Kavanagh, B. Ziółkowski, L. Florea, D. R. MacFarlane, K. Fraser and D. Diamond, *Physical Chemistry Chemical Physics*, 2013, **16**, 3610.

24. M. R. Guilherme, R. da Silva, A. F. Rubira, G. Geuskens and E. C. Muniz, *Reactive & Functional Polymers*, 2004, **61**, 233-243.

25. M. Hammarson, J. R. Nilsson, S. Li, T. Beke-Somfai and J. Andréasson, *The Journal of Physical Chemistry B*, 2013, **117**, 13561-13571.

26. L. Ionov, *Materials Today*, 2014, **17**, 494-503.

27. Y. Kohno, Y. Deguchi and H. Ohno, *Chemical Communications*, 2012, **48**, 11883-11885.

28. Y. Kohno and H. Ohno, *Australian Journal of Chemistry*, 2012, **65**, 91-94.

29. Y. Kohno, S. Saita, Y. Men, J. Yuan and H. Ohno, *Polymer Chemistry*, 2015, 2163-2178.

30. J. Yuan, D. Mecerreyes and M. Antonietti, *Progress in Polymer Science*, 2013, **38**, 1009-1036.

31. B. Ziółkowski and D. Diamond, *Chemical Communications*, 2013, **49**, 10308-10310.

32. B. Ziółkowski, L. Florea, J. Theobald, F. Benito-Lopez and D. Diamond, *Soft Matter*, 2013, **9**, 8754.

33. Y. Maeda, T. Higuchi and I. Ikeda, *Langmuir*, 2001, **17**, 7535-7539.

34. H. G. Schild, *Progress in Polymer Science*, 1992, **17**, 163-249.

35. X. Z. Zhang, Y. Y. Yang, T. S. Chung and K. X. Ma, *Langmuir*, 2001, **17**, 6094-6099.

36. T. Glennon, J. Saez, M. Czugala, L. Florea, E. McNamara, K. J. Fraser, J. Ducree, D. Diamond and F. Benito-Lopez, *ieee*, 2015, 109-112.

37. F. Benito-Lopez, R. Byrne, A. M. Răduţă, N. E. Vrana, G. McGuinness and D. Diamond, *Lab on a Chip*, 2010, **10**, 195-201.

38. S. Sugiura, K. Sumaru, K. Ohi, K. Hiroki, T. Takagi and T. Kanamori, *Sensors and Actuators A: Physical*, 2007, **140**, 176-184.

39. N. S. Satarkar, W. Zhang, R. E. Eitel and J. Z. Hilt, *Lab on a Chip*, 2009, **9**, 1773-1779.

40. S. Ghosh, C. Yang, T. Cai, Z. Hu and A. Neogi, *Journal of Physics D: Applied Physics*, 2009, **42**, 135501.

41. G. Vancoillie, D. Frank and R. Hoogenboom, *Progress in Polymer Science*, 2014, **39**, 1074-1095.

42. D. Mecerreyes, *Progress in Polymer Science*, 2011, **36**, 1629-1648.

43. F. Benito-Lopez, M. Antoñana-Díez, V. F. Curto, D. Diamond and V. Castro-López, *Lab on a Chip*, 2014, **14**, 3530-3538.

44. M. Yoshizawa and H. Ohno, *Electrochimica Acta*, 2001, **46**, 1723-1728.

45. A. S. Shaplov, E. I. Lozinskaya, D. O. Ponkratov, I. A. Malyshkina, F. Vidal, P.-H. Aubert, O. g. V. Okatova, G. M. Pavlov, L. I. Komarova, C. Wandrey and Y. S. Vygodskii, *Electrochimica Acta*, 2011, **57**, 74-90.

46. M. Koebe, M. Drechsler, J. Weber and J. Yuan, *Macromolecular Rapid Communications*, 2012, **33**, 646-651.

47. S. Gallagher, L. Florea, K. Fraser and D. Diamond, *International Journal of Molecular Sciences*, 2014, **15**, 53375349.
48. A. Tudor, L. Florea, S. Gallagher, J. Burns and D. Diamond, *Sensors*, 2016, **16**, 219.
49. B. Ziółkowski, Z. Ates, S. Gallagher, R. Byrne, A. Heise, K. J. Fraser and D. Diamond, *Macromolecular Chemistry and Physics*, 2013, **214**, 787796.
50. Y. Men, H. Schlaad, A. Voelkel and J. Yuan, *Polymer Chemistry*, 2014, **5**, 3719-3724.
51. Y. Tanaka, T. Fujikawa, Y. Kazoe and T. Kitamori, *Sensors and Actuators B: Chemical*, 2013, **184**, 163-169.
52. C. H. Zhu, Y. Lu, J. Peng, J. F. Chen and S. H. Yu, *Advanced Functional Materials*, 2012, **22**, 4017-4022.
53. E. Lee, H. Lee, S. I. Yoo and J. Yoon, *ACS applied materials & interfaces*, 2014, **6**, 16949-16955.

**Vitae**

**Alexandru Tudor** is a PhD student in Prof. Dermot Diamond's research group at Dublin City University. He graduated from the University "Politehnica" of Timisoara, Romania with a M. Sc. in Micro and Nanomaterials, and the West University of Timisoara, Romania with a B. Sc. in Chemistry. Alexandru's PhD programme is part of the OrgBIO FP7 project. His research focuses on the synthesis and characterization of poly(ionic liquid)s for use as smart polymers and functional materials in organic bioelectronics.

**Janire Saez** has a M.Sc. in chemistry (2012) and a postgraduate master in Pharmacology (2013) from the University of the Basque Country UPV/EHU in Spain. In 2015 she joined the Microfluidics Cluster UPV/EHU where is currently doing her PhD studies. Her research interests are focused on the integration of smart materials into environmentally friendly microfluidic devices.

**Dr. Larisa Florea** studied organic chemistry and chemical engineering at University "Politehnica" from Timisoara, Romania (B.Sc. Hons 2009). In 2009 she joined the Adaptive Sensors Group at Dublin City University where she earned her Ph.D. under the supervision of Prof. Dermot Diamond and Dr. Fernando Benito-Lopez. Since 2013 she has carried out her postdoctoral research with Prof. Dermot Diamond in the INSIGHT Centre at Dublin City University, where she is currently Team Leader in smart materials and microfluidics. Her research interests include the design, synthesis and applications of stimuli-responsive polymers as novel sensing and actuating materials in microfluidic devices.

**Dr. Fernando Benito-Lopez** studied chemistry at the Universidad Autonoma de Madrid and completed his master studies in the Department of Inorganic Chemistry in 2002. He obtained his PhD at the University of Twente, The Netherlands, in 2007. He carried out his postdoctoral research in the group of Prof. Dermot Diamond at Dublin City University, Dublin, where in 2010, he became Team Leader in polymer microfluidics. In 2012 he moved to CIC microGUNE a Research Centre working in Microtechnology in Spain. From 2015 he is Ramón y Cajal Fellow and leader of the Microfluidics Cluster UPV/EHU at the University of the Basque Country, Spain.

**Prof. Dermot Diamond** received his Ph.D. and D.Sc. from Queen's University Belfast (Chemical Sensors, 1987, Internet Scale Sensing, 2002), and was Vice-President for Research

at Dublin City University (2002–2004). He has published over 300 peer-reviewed papers in international journals, is a named inventor in 18 patents, and is co-author and editor of four books. He is director and founding member of the National Centre for Sensor Research (www.ncsr.ie) at Dublin City University, and an SFI-funded investigator in the INSIGHT Centre (http://www.insight-centre.org).
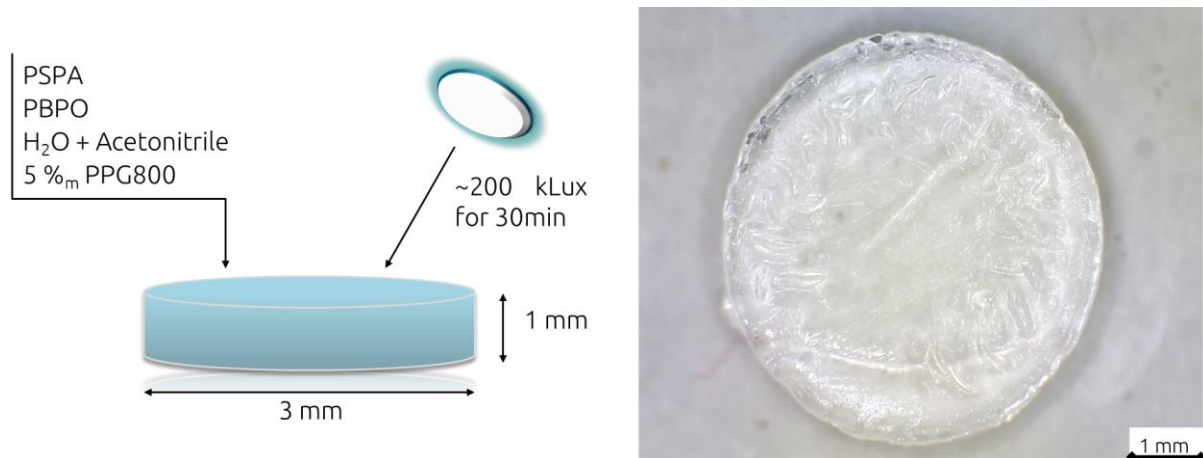
Fig. 1. Schematic illustration of PSPA hydrogel disk polymerization protocol (left) and photo of the PSPA hydrogel disk (right).
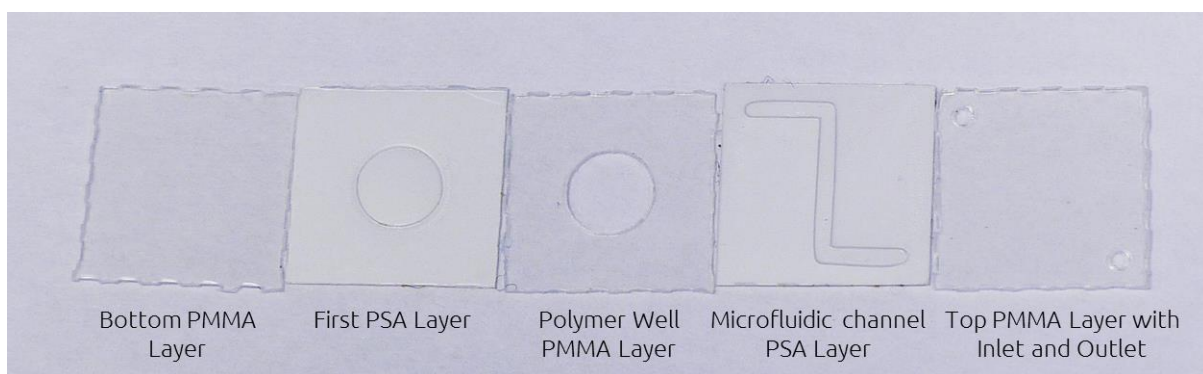


Fig. 2. PMMA and PSA layers of the microfluidic chip before assembly.
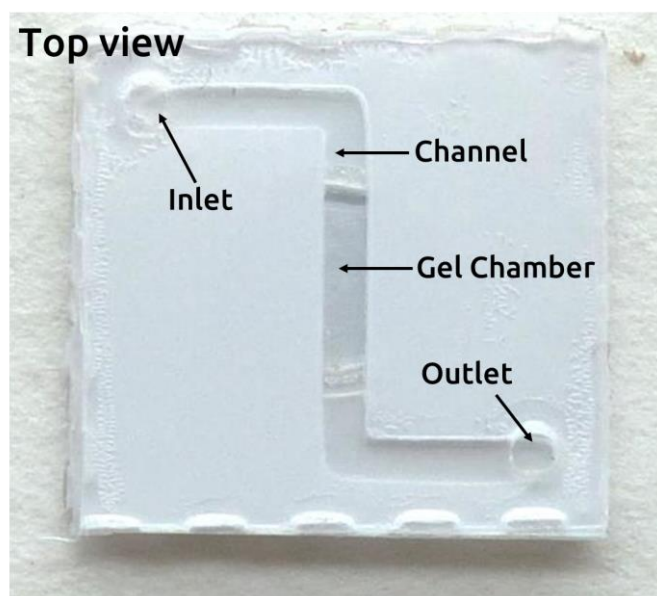
Fig. 3. The assembled microfluidic chip containing the thermo-responsive hydrogel actuator.
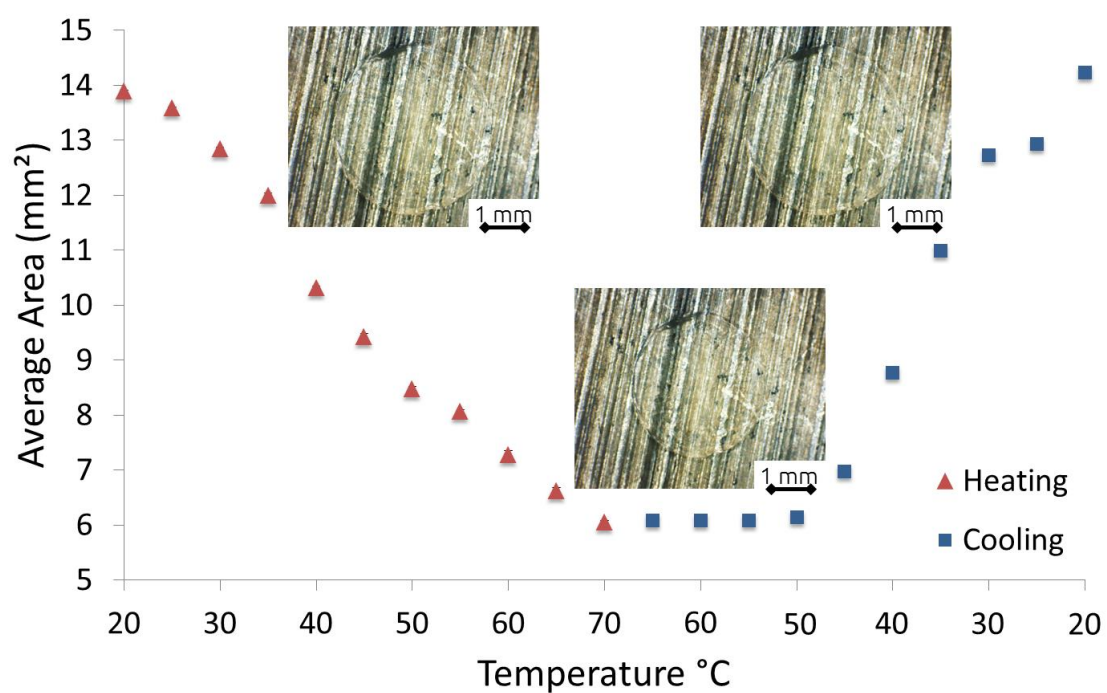


Fig. 4. Shrinking and reswelling behaviour of the PSPA hydrogels when the temperature is increased from 20 °C to 70 °C, followed by decreasing it back to 20 °C, in 5 °C steps.
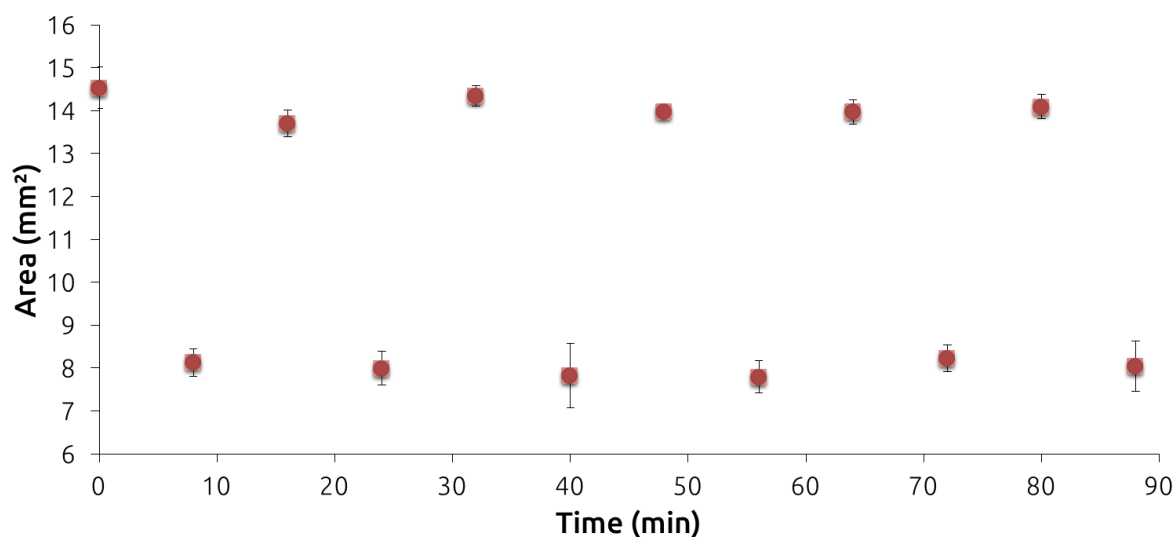
Fig. 5. Temperature-induced shrinking by area of the PSPA hydrogels at 20 °C and at 50 °C.
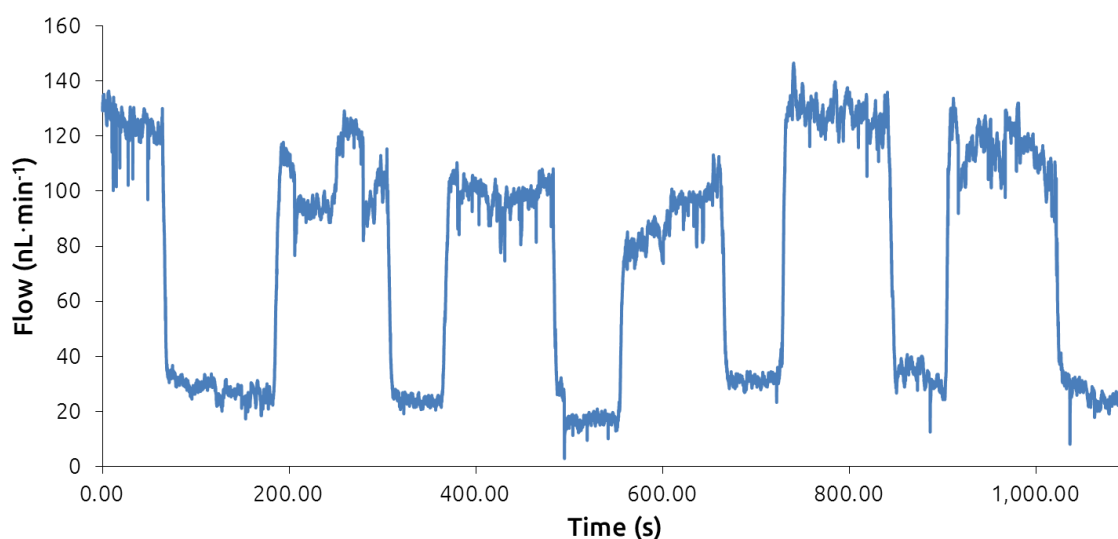


Fig. 6. PSPA hydrogel actuator at 50 °C allowing a flow rate of ~ 140 nL·min$^{-1}$ to pass through the microfluidic channel, and, at 20 °C, restricting flow rate to ~ 20 nL·min$^{-1}$. Small fluctuations on the signal (10 ± 5 nL·min$^{-1}$) were observed due to ambient conditions (*e.g.* vibration of the pumping system) and the ionic liquid polymer network internal reorganisation before and after temperature actuation, which is extended after the stimulus is removed due to the hydration or dehydration processes that continue to happen in the polymer.
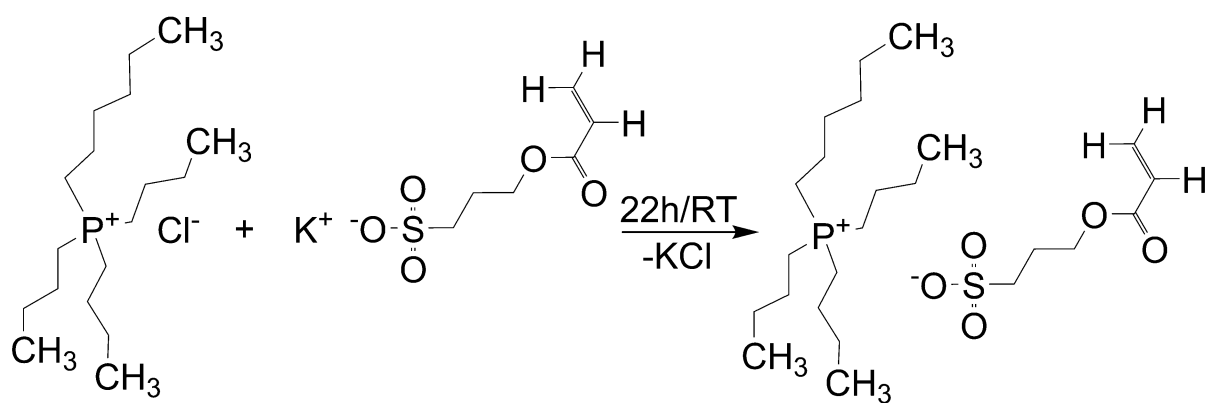
Scheme 1. Reaction scheme for PSPA synthesis.
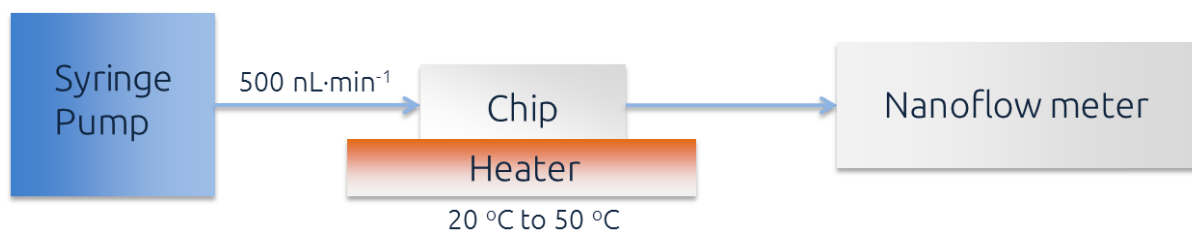


Scheme 2. Setup used for the characterization of DI water flow through the chip.

Table 1. Experimental shrinking and swelling rate constants.

| Shrinking | | Swelling | |
|---|---|---|---|
| **Repetition** | k | **Repetition** | k |
| 1 | 0,9 | 1 | 0,9 |
| 2 | 0,4 | 2 | 0,9 |
| 3 | 0,5 | 3 | 0,8 |
| 4 | 0,8 | 4 | 0,4 |
| 5 | 0,7 | 5 | 0,5 |
| 6 | 0,6 | | |
| **Average** | 0,6 | **Average** | 0,7 |
| **Standard Deviation** | 0,2 | **Standard Deviation** | 0,3 |
| **RSD (%)** | 29,8 | **RSD (%)** | 36,4 |